Effective Interaction Parameter for Homologous Series of Deuterated Polystyrene-*block*-Poly(*n*-alkyl methacrylate) Copolymers

Du Yeol Ryu,[†] Changhak Shin,[†] Junhan Cho,*[,‡] Dong Hyun Lee,[§] Jin Kon Kim,*[,§] Kristopher A. Lavery,[||] and Thomas P. Russell[||]

Department of Chemical Engineering, Yonsei University, 134 Sinchon-dong, Seodaemun-gu, Seoul 120-749, Korea, Department of Polymer Science & Engineering, and Hyperstuructured Organic Materials Research Center, Dankook University, San-8, Hannam-dong, Yongsan-gu, Seoul 140-714, Korea, National Creative Research Initiative Center for Block Copolymer Self Assembly, Department of Chemical Engineering and Polymer Research Institute, Pohang University of Science and Technology, Kyungbuk, 790-784, Korea, and Department of Polymer Science and Engineering, University of Massachusetts, Amherst, Massachusetts 01003

Received March 29, 2007; Revised Manuscript Received July 7, 2007

ABSTRACT: The effective interaction parameters, (χ_F) of the homologous series of deuterated polystyrene-*block*-poly(*n*-alkyl methacrylate) copolymers (dPS-*b*-PA$_n$MA) from methyl ($n = 1$) to hexyl ($n = 6$) side groups have been investigated by small-angle neutron scattering and a Hartree (fluctuation correction) analysis. While χ_F for dPS-*b*-PA$_n$MA with $n = 1$ and 6 is a typical decreasing function of temperature, it is shown that χ_F for n from 2 to 4 changes to a monotonic increase with temperature, revealing growing upward convexity. This action culminates in a maximum of χ_F for $n = 5$, which suggests an immiscibility loop-type behavior. Using the Hartree analysis for compressible diblock copolymers, the effect of directional interactions and the compressibility difference between the constituent blocks on χ_F is discussed. The ordering transition temperatures, their pressure dependences, and χ_F for the homologous block copolymer series are shown to be in good agreement with the experimental values.

1. Introduction

Block copolymers have received considerable attention since they self-assemble into arrays of ordered nanoscopic structures.[1−3] The phase behavior of a block copolymer is determined by composition such as volume fraction, total number of monomers N, and the Flory−Huggins interaction parameter χ_F.[4] Block copolymers generally exhibit ordering upon cooling, which is referred to as the order−disorder transition (ODT).[3,5] Most theoretical analyses on block copolymers are based on the assumption of the incompressibility.[2,4] However, there have been numerous recent findings that demonstrate a clear need to incorporate compressibility into theoretical arguments to explain the response of block copolymers to pressure. Relevant findings include the observed ordering of block copolymers upon heating, which is referred to as the lower disorder−order transition (LDOT),[6−11] baroplasticity that is used for pressure-induced processing,[12−16] and the observation of immiscibility loops.[14,17−19]

The LDOT and the effect of pressure on the ordering transition have been successfully described in recent studies using the Landau and Hartree (fluctuation correction) approaches, which are based on a compressible random-phase approximation (RPA) theory developed by one of the authors.[20−26] Finite compressibility was incorporated into the theory through effective RPA interactions, which is obtained from a molecular equation-of-state model by Cho and Sanchez (CS).[20,27] The χ_F was reinterpreted as $\chi_F = \chi_{app} + \chi_{comp}$, where χ_{app} is the conventional exchange energy with proper density dependence and χ_{comp} represents compressibility difference between constituent blocks. Many block copolymers with positive (unfavorable) exchange energy contributions to χ_{app} would experience typical ODT behavior. However, some block copolymers with directional interactions would develop growing unfavorable exchange energy contributions to χ_{app} with temperature, due to the entropic penalty of forming such directional pairs. Other block copolymers with large compressibility difference and, thus, large χ_{comp} would gain more entropy due to the increased volume when they phase separate. Such entropic driving forces can induce LDOT behavior.

It was reported that the phase behavior of the homologous series of polystyrene-*block*-poly(*n*-alkyl methacrylate) copolymers (PS-*b*-PA$_n$MA) changed dramatically with the carbon number n of the alkyl groups.[6−8,12−14,17,18,28−31] PS-*b*-PA$_n$MA with $n = 1$ or $n \geq 6$, where the difference in the solubility parameter δ between blocks is appreciable, exhibits common ODT behavior. PS-*b*-PA$_n$MA with $n = 2$ to 4, on the other hand, exhibits LDOT behavior, where δ's of the constituent blocks are quite close.[6,7,13,29,32] PS-*b*-PA$_5$MA showed an immiscibility loop with both LDOT and upper ODT.[14,17,18,30−32] The pressure dependence of the observed transitions for PS-*b*-PA$_n$MA is quite varied. It was observed by the superposition of scattering intensities at elevated pressures that the ODT-type PS-*b*-PA$_1$-MA reveals ordering upon pressurization (barotropicity) with a dependence of the transition temperature on pressure, $\Delta T/\Delta P$, of +23 K/100 MPa.[13] PS-*b*-PA$_6$MA, on the other hand, disorders upon pressurization (baroplasticity) with $\Delta T/\Delta P$ of −60 K/100 MPa.[13] All of the LDOT-type block copolymers show baroplasticity. For $n = 2$, 3, and 4, $\Delta T/\Delta P$ of their LDOT's are respectively 100, 90, and 147 K/100 MPa.[12,13] By direct

* To whom correspondence should be addressed. E-mail: (J.C.) jhcho@dku.edu; (J.K.K.) jkkim@postech.ac.kr.
[†] Department of Chemical Engineering, Yonsei University.
[‡] Department of Polymer Science & Engineering, and Hyperstuructured Organic Materials Research Center, Dankook University.
[§] National Creative Research Initiative Center for Block Copolymer Self Assembly, Department of Chemical Engineering and Polymer Research Institute, Pohang University of Science and Technology.
[||] Department of Polymer Science and Engineering, University of Massachusetts, Amherst.

10.1021/ma070754z CCC: $37.00
Published on Web 09/14/2007

Table 1. Sample Characteristics for dPS-*b*-PA$_n$MA Used Here

polymers	M^a	polydispersity^a	Φ_{dPS}	$\langle N_e \rangle^b$	
dPS-*b*-PA$_1$MA	19 800	1.02	0.500	186.8	homogeneous
dPS-*b*-PA$_2$MA	82 500	1.02	0.504	729.0	homogeneous
	99 000	1.02	0.501	874.8	exhibiting LDOT
dPS-*b*-PA$_3$MA	75 300	1.02	0.515	627.3	homogeneous
	119 600	1.02	0.510	997.1	exhibiting LDOT
	135 000	1.02	0.499	1125.5	exhibiting LDOT
dPS-*b*-PA$_4$MA	47 200	1.03	0.501	373.1	homogeneous
	55 200	1.02	0.485	436.9	exhibiting LDOT
dPS-*b*-PA$_5$MA	46 000	1.03	0.500	347.1	homogeneous
	50 000	1.04	0.500	377.4	exhibiting loop (LDOT+ODT)
dPS-*b*-PA$_6$MA	25 300	1.01	0.500	182.7	homogeneous
	37 000	1.03	0.500	267.5	exhibiting ODT

[a] M, which denotes the number-average molecular weight, and the polydispersity were measured by SEC coupled with multiangle laser light scattering. [b] To determine N_e, $\upsilon_{sp,dPS} = 0.87$ cm^3/g is used, and $\upsilon_{sp,PAnMA}$ for n from 1 (methyl) to 6 (n-hexyl) is taken as 0.845, 0.889, 0.926, 0.952, 0.970, and 0.994 cm^3/g referred at room temperature, respectively.

measurement of the transition temperatures at elevated pressures, $\Delta T/\Delta P$ of PS-*b*-PA$_5$MA was unprecedentedly large as 725 K/100 MPa and −725 K/100 MPa for LDOT and upper ODT, respectively.[14]

Prior to the discovery of loop forming PS-*b*-PA$_5$MA, the LDOT and baroplastic character of PS-*b*-PA$_n$MA has been attributed to differences in monomer structures by Freed and co-workers in their lattice cluster model[32] or to differences in pure component properties by Ruzette and Mayes in a simple phenomenological model.[33,34] However, it is perceived that the unique behavior of PS-*b*-PA$_5$MA is key to understanding the phase behavior of the homologous series. Two key features are the maximum in χ_F as a function of temperature and the unprecedentedly large value of $\Delta T/\Delta P$. By using the recently developed Hartree analysis, incorporating directional interactions, for compressible block copolymers,[22,23] we provide here a unified view of the phase behavior for a series of deuterated PS-*b*-PA$_n$MA copolymers. As deuteration can affect the phase behavior of given mixture systems,[35] the transition temperatures as well as $\Delta T/\Delta P$ of the deuterated PS-*b*-PA$_n$MA samples employed here are newly measured. It is shown that suitable values of parameters, like self- and cross-interaction parameters, monomer diameters, and chain sizes, give predictions of χ_F and $\Delta T/\Delta P$ that agree with experimental findings.

2. Experimental Section

Deuterated polystyrene-*block*-poly(*n*-alkyl methacrylate) copolymers, denoted as dPS-*b*-PnA$_n$MA, with symmetric composition, were synthesized by the sequential anionic polymerization of *d*-styrene and *n*-alkyl methacrylate in tetrahydrofuran (THF) at −78 °C in the presence of LiCl under purified Ar using *sec*-BuLi as an initiator. LiCl (high purity, Aldrich) was dried overnight at 150 °C under vacuum and then dissolved in dried THF. Refluxed THF from CaH_2 was stirred over fresh sodium−benzophenone complex until it showed a deep purple color, indicating an oxygen- and moisture-free solvent. Degassed monomers with CaH_2, deuterated styrene (99.5%, CDN isotopes) and *n*-alkyl methacrylates (high purity, Aldrich and Scientific Polymer Products Inc.) were vacuum-distilled over dried dibutyl magnesium and trioctyl aluminum, respectively, until a persistent characteristic color was observed: yellow for dPS and yellowish green for PnA$_n$MA. It took 1 h to synthesize *d*-styrene for full conversion. A small quantity of first polymerized block was transferred into a tube and then terminated with purified 2-propanol to determine the molecular weight of dPS block. After alkyl methacrylate monomer was introduced very slowly into the reactor and then stirred for 5 h, the polymer solution, terminated with purified 2-propanol, was precipitated in methanol/water (80/20 wt/wt) mixture.

The weight and number-average molecular weights were measured by size exclusion chromatography (SEC) coupled with multiangle laser light scattering. The polydispersity index of all dPS-*b*-PnA$_n$MA's synthesized was less than 1.03. The volume fractions of the dPS block in all block copolymers were ∼0.5 as determined by nuclear magnetic resonance. The molecular characteristics of dPS-*b*-PnA$_n$MA's used in this study are given in Table 1.

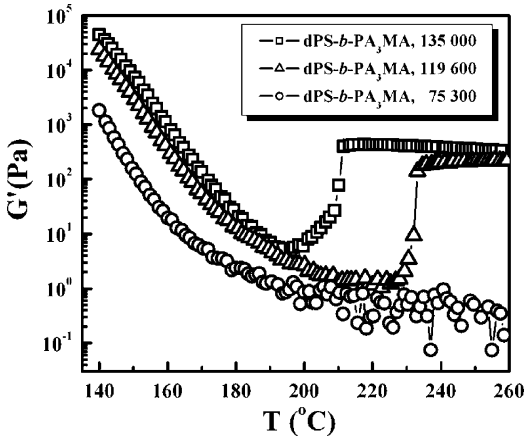

Figure 1. Temperature dependence of G'(Pa) for three symmetric dPS-*b*-PA$_3$MA's: M = 135000, 119600, and 75300.

SANS experiments were performed at the HANARO (Korea) and IPNS (Argonne National Lab). Scattering intensities were collected on a 2-D area detector and then circularly averaged. The sample thickness was 1 mm and the exposure time was 1 h. The samples were equilibrated for 1 h at each temperature before measurement. SANS profiles at temperatures greater than 120 °C were obtained at every 10 °C or selected temperature during heating. Samples were prepared by compression molding, followed by annealing at a temperature well above glass transition temperature (T_g) under vacuum for 24 h.

An Advanced Rheometric Expansion System (Rheometrics Co.) with 25 mm diameter parallel plates was also used to determine the temperature dependence of shear modulus (G') of dPS-*b*-PnA$_n$-MA from 115 to 265 °C at a heating rate of 0.5 °C/min. A strain amplitude of 0.05 and angular frequency of 0.1 rad/s, which lie in the linear viscoelastic regime, were used.

Birefringence under elevated hydrostatic pressures was measured to obtain the pressure coefficients of transition temperatures, which were alternatively taken with SANS as well. Vertically polarized light from a He−Ne laser with a wavelength of 632.8 nm passes through the sample and a horizontal analyzing polarizer onto a photodiode.[19]

3. Results and Discussion

3.1. Pressure Dependence of Transition Temperatures for dPS-*b*-PA$_n$MA's. Figure 1 shows a temperature sweep of G' for symmetric dPS-*b*-PA$_3$MA's with the indicated molecular

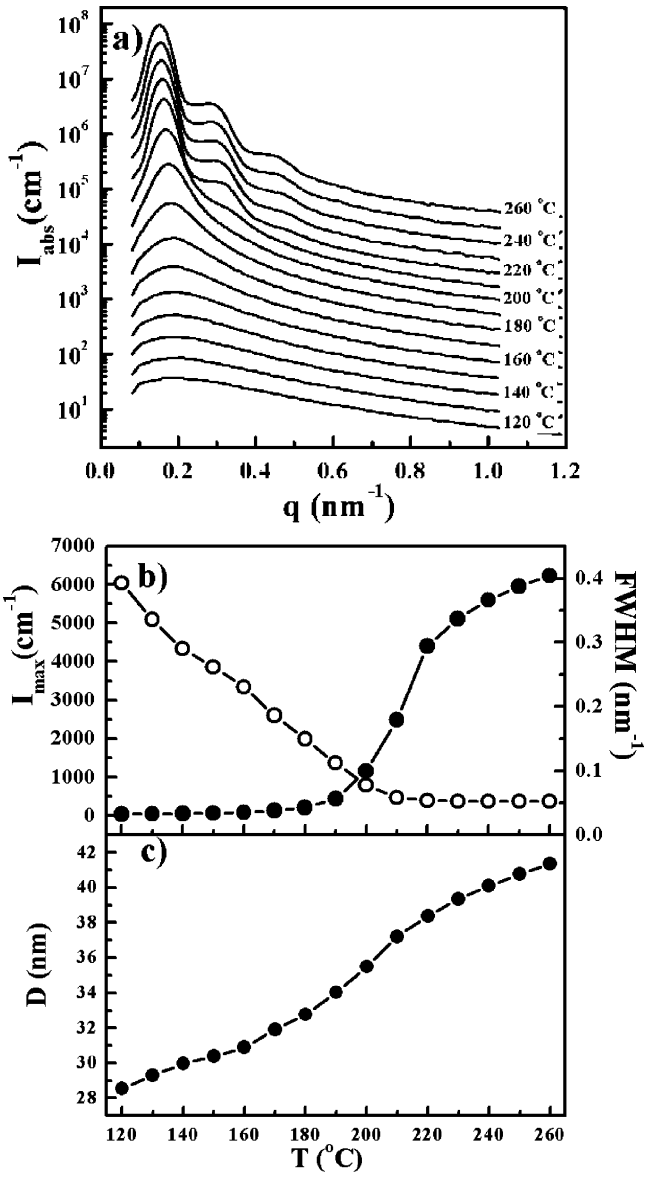

Figure 2. (a) Absolute intensity (I_{abs}) for dPS-*b*-PA$_3$MA of M = 135 000 at various temperatures. (b) Temperature dependence of maximum intensity (I_{max}; ●), fwhm (○), and (c) domain spacing ($D = 2\pi/q^{max}$).

weights. The G' for dPS-*b*-PA$_3$MA of molecular weight M = 75 300 decreases gradually with increasing temperature, indicating that this block copolymer is phase-mixed over the entire temperature range. When the molecular weight is increased to 119600, G' first decreases but increases rapidly at 225 °C, and the higher value of G' is maintained at higher temperatures, suggesting that this block copolymer undergoes ordering with increasing temperature. With a further increase in M to 135 000, the transition temperature was shifted to 195 °C. This type of ordering transition is the lower disorder to order transition (LDOT), consistent with the previous report by Ruzette et al.[7]

Figure 2a shows the SANS profiles (the absolute scattering intensity $I_{abs}(q)$ vs q, where q is the scattering vector given by $(4\pi/\lambda)$ sin θ with 2θ and λ denoting scattering angle and wavelength, respectively) for dPS-*b*-PA$_3$MA of M = 135000 at various temperatures from 120 to 260 °C. The weak maximum in I_{abs} at lower temperatures sharpens with increasing temperature, and higher-order reflections, characteristic of lamellar microdomain morphology, are observed. The LDOT was taken to be 193 °C from plots of the maximum intensity (I_{max}), full width at half-maximum (fwhm), and domain spacing (D), where $D = 2\pi/q^{max}$, as given in Figure 2, parts b and c. This result is essentially the same as that determined from G'. The transition temperatures for all other dPS-*b*-PnA$_n$MA were determined similarly and are summarized in Table 2.

Figure 3a gives SANS profiles at various hydrostatic pressures and at 230 °C for dPS-*b*-PA$_3$MA of M = 135 000. At 1.38 MPa, a sharp primary peak as well as higher-order reflections is seen, indicating that the block copolymer exhibits a lamellar morphology at lower pressures. When pressure is increased to 82.7 MPa, however, a single broad peak with reduced intensity is seen, which can be attributed to a correlation hole scattering, indicating that the block copolymer becomes disordered at this pressure. The temperature dependence of I_{max} and the fwhm for the primary reflection are given in Figure 3, parts b and c, at elevated pressures. It was found that T_{LDOT} at a given pressure is easily determined from the sharp transition in I_{max}. With increasing pressure, T_{LDOT} shifted to higher temperatures, which indicates the enhanced miscibility between dPS and PA$_3$MA upon pressurization.

From the changes in the T_{LDOT} with pressure, as shown in Figure 4, $\Delta T_{LDOT}/\Delta P$ for dPS-*b*-PnA$_3$MA is determined to be 62.2 °C/100 MPa. This value is slightly smaller than that given in ref 13. It should be noted that PS-*b*-PA$_3$MA (not dPS-*b*-PA$_3$-MA) was used in ref 13, and $\Delta T_{LDOT}/\Delta P$ was estimated from the shift of scattering intensity curves to that at a reference temperature, whereas in this study it was obtained by directly measuring T_{LDOT} with elevated pressures. For all other dPS-*b*-PA$_n$MA's, the values of $\Delta T/\Delta P$ are summarized in Table 2. The dPS-*b*-PA$_1$MA copolymer possesses a small and positive (barotropic) $\Delta T_{ODT}/\Delta P$ of +23 °C/100 MPa,[13] because the repulsive interaction between the two blocks strengthens upon pressurization. For dPS-*b*-PA$_n$MA with n = 2 to 5, the ordering is suppressed and baroplasticity is seen with $\Delta T_{LDOT}/\Delta P$ of +62 to +725, depending on n, which is attributed to the suppression of compressibility effects in their ordering behavior. It is shown that $\Delta T_{LDOT}/\Delta P$ for dPS-*b*-PA$_4$MA in ref 12 is slightly smaller than that in this study, which was obtained for hydrogeneous PS-*b*-PA$_4$MA of M = 60 300. dPS-*b*-PA$_6$MA, despite its ODT character, reveals the negative (baroplastic) $\Delta T_{ODT}/\Delta P$ of −115 °C/100 MPa, which is then slightly larger in its absolute value than that for PS-*b*-PA$_6$MA in ref 13. These results imply that deuteration effects are indeed not strong enough to substantially change the nature of phase behavior in these dPS-*b*-PA$_n$MA copolymers, and all the data measured here are consistent with those previously reported.[12,13]

3.2. SANS Measurements for Disordered dPS-*b*-PA$_n$MA's. SANS measurements on lower molecular weight dPS-*b*-PA$_n$-MA's indicated that all the block copolymers were in the disordered state over the entire temperature range. This allows us to obtain the effective interaction parameters between dPS and PA$_n$MA depending on n. The SANS profiles could be described using an empirical effective interaction parameter $\chi_L(T)$ by fitting $I(q)$ to the Leibler's incompressible scattering function $S(q)$.[4] The absolute intensity (I_{abs} in cm^{-1}) is given by

$$I_{abs}(q) = \upsilon_{ref}\left(\frac{b_1}{\upsilon_1} - \frac{b_2}{\upsilon_2}\right)^2 \times S(q) \qquad (1)$$

where b_i is the coherent neutron scattering length and υ_i is the monomeric volume for the ith component. The reference volume υ_{ref} is defined as

$$\upsilon_{ref} = (\upsilon_{sp,dPS}[M]_{o,dPS} * \upsilon_{sp,PnAMA}[M]_{o,PnAMA})^{1/2} \qquad (2)$$

Table 2. Experimental Transition Temperatures and Their Pressure Coefficients for the Symmetric dPS-*b*-PA$_n$MA's

polymers	M (g/mol)	type	transition (°C) at 0.1 MPa	$\Delta T/\Delta P$ (°C /100 MPa)	$\Delta T/\Delta P$[a] (°C /100 MPa)
dPS-*b*-PA$_1$MA	22 160	ODT	120[b]		+23[c]
dPS-*b*-PA$_2$MA	99 000	LDOT	225[d] (225[e])	+99[f]	+100[c]
dPS-*b*-PA$_3$MA	119 600	LDOT	225[d]		
	135 000		195[d] (193[e])	+62[e]	+90[c]
dPS-*b*-PA$_4$MA	55 200	LDOT	170[e]	+195[g]	+147[h]
dPS-*b*-PA$_5$MA	50 000	LDOT + ODT	165, 245[i]	+725, −725[j]	
dPS-*b*-PA$_6$MA	37 000	ODT	160[e]	−115[f]	−60[c]

[a] The previously reported data in ref 12 and 13. [b] Extrapolated from χ_L data. [c] Data from ref 13. [d] Determined by rheology measurements. [e] By SANS measurements. [f] By birefringence measurements. [g] Hydrogeneous PS-*b*-PA$_4$MA with M = 60 300 was used in the birefringence measurements. [h] Data from ref 12. [i] From ref 30. [j] From ref 14.

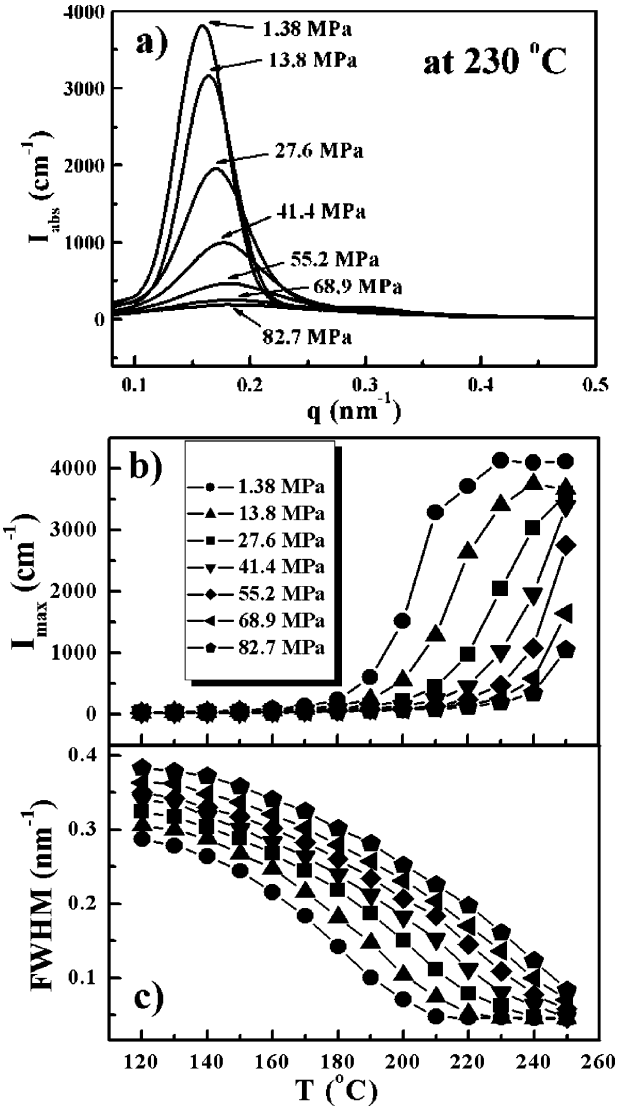

Figure 3. (a) Absolute intensity (I_{abs}) for dPS-*b*-PA$_3$MA of M = 135 000 at various hydrostatic pressures with constant temperature (T = 230 °C). Temperature dependence of (b) maximum intensity (I_{max}) and (c) fwhm at various hydrostatic pressures.

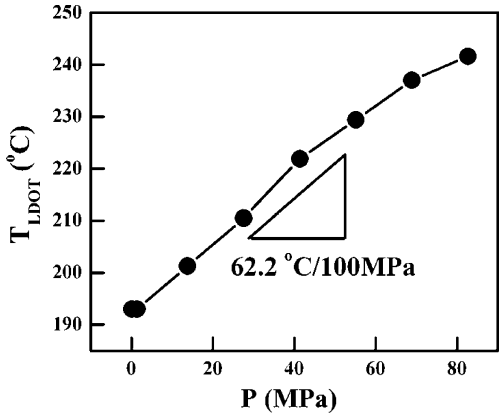

Figure 4. Changes of T_{LDOT} for dPS-*b*-PA$_3$MA of M = 135 000 with hydrostatic pressure measured by SANS.

where $v_{sp,i}$ and $[M]_{o,i}$ are the specific volume (cm^3/g) and the monomer molecular weight of the ith component, respectively. The scattering function, $S(q)$, of a diblock copolymer melt is given as follows:

$$S(q)^{-1} = \frac{S_{11}{}^0 + S_{22}{}^0 + 2S_{12}{}^0}{N_e \det[S_{ij}{}^0]} - 2\chi_L \qquad (3)$$

Here S_{ij}^0 is the i,j-correlation function for incompressible Gaussian A-*b*-B chains. From the experiment, the total number of segments (N_e) is defined as $N_e = (V_{dPS} + V_{PnAMA})/v_{ref}$, where V_{dPS} and V_{PnAMA} are, respectively, the molar volumes of the dPS and poly(*n*-alkyl methacrylate) blocks. The footnote of Table 1 lists the specific volumes of deuterated styrene and *n*-alkyl methacrylate monomers.

Figure 5a gives the SANS profiles for dPS-*b*-PA$_1$MA of M = 19 800 at various temperatures from 120 to 260 °C. Weak, broad maxima in I_{abs} are observed due to the correlation hole scattering of the block copolymer in the disordered state. As shown in Figure 5b, I_{max} decreases (but fwhm increases) gradually with increasing temperature, indicating typical ODT behavior for block copolymers. The values of χ_L obtained for dPS-*b*-PA$_1$MA are shown in Figure 5c as a function of temperature. It is seen that χ_L decreases with increasing temperature.[36] This result agrees with the temperature dependence of I_{max}, i.e., the typical phase behavior of block copolymers with an ODT.

Figure 6a gives SANS profiles for dPS-*b*-PA$_6$MA of M = 25 300. I_{max} decreases and the fwhm increases with temperature, as shown in Figure 6, parts b and c. Consequently, the behavior of I_{max} and fwhm with temperature shows the same trend as dPS-*b*-PA$_1$MA. χ_L, obtained from this analysis, as a function of temperature is shown in Figure 6c. It is seen that χ_L decreases with increasing temperature, signifying an ODT.[36]

dPS-*b*-PA$_2$MA with M = 82 500 and dPS-*b*-PA$_3$MA of M = 75 300, however, exhibited a completely different phase behavior, as shown in Figures 7 and 8. For these block copolymers, a broad maximum arising from the correlation hole scattering of the block copolymer in the disordered state is shown in Figures 7a and 8a. Although a relatively intensified peak is seen at higher temperatures for dPS-*b*-PA$_2$MA, the block copolymer was disordered over the entire experimental tem-

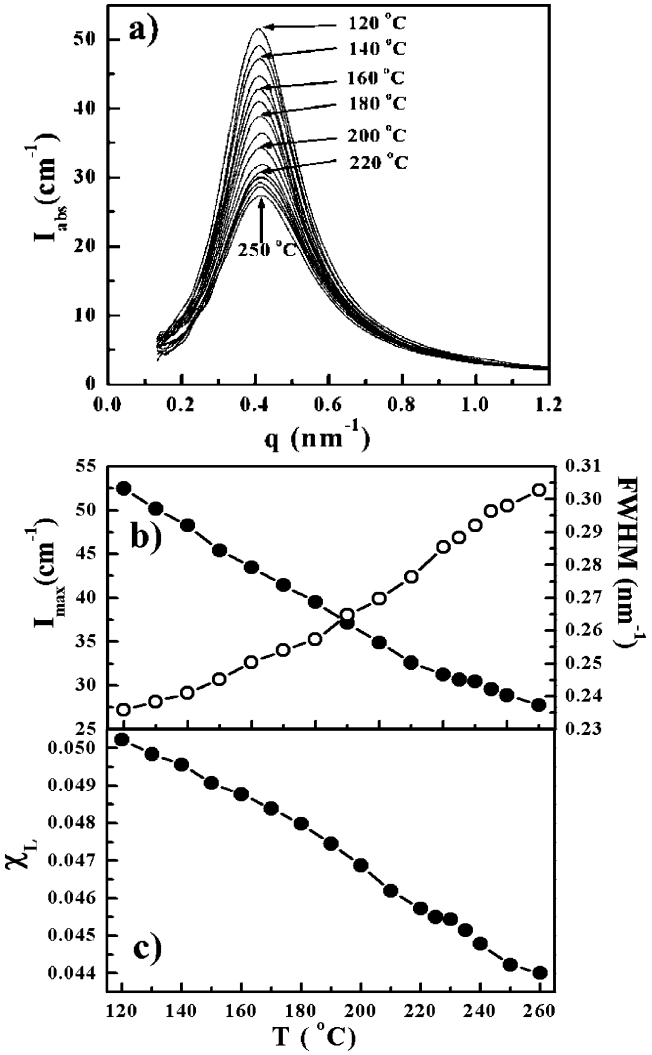

Figure 5. (a) Absolute intensity (I_{abs}) for dPS-*b*-PA$_1$MA of $M = 19\,800$ at various temperatures. (b) Temperature dependence of maximum intensity (I_{max}; ●), fwhm (○), and (c) empirical interaction parameter (χ_L).

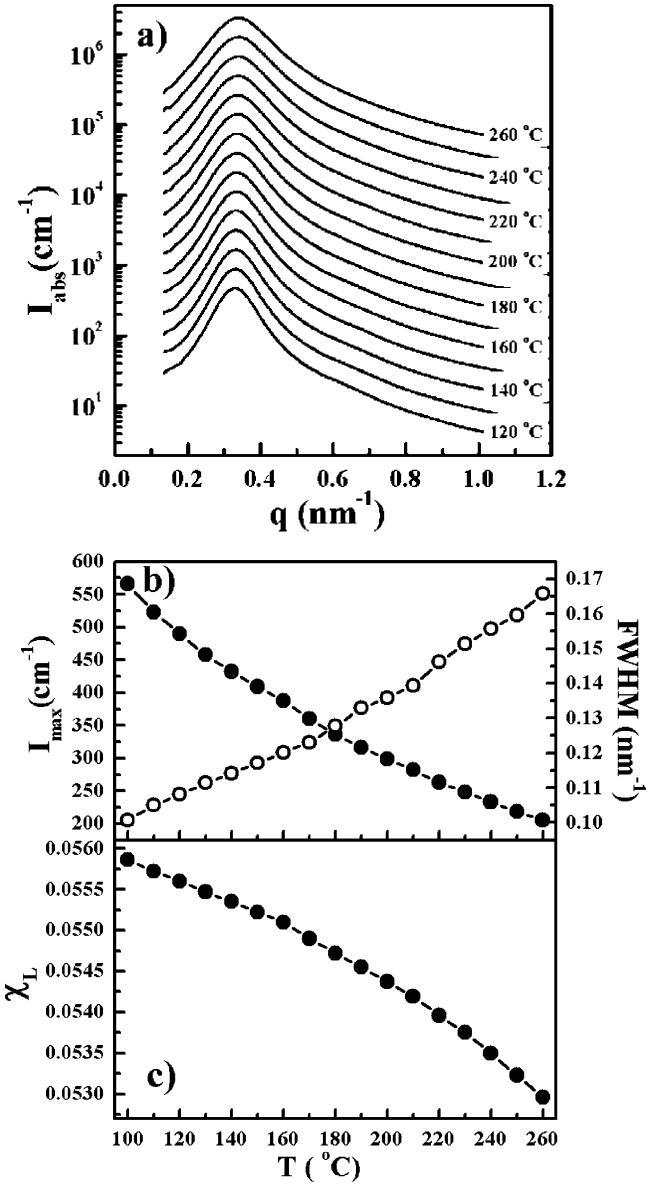

Figure 6. (a) Absolute intensity (I_{abs}) for dPS-*b*-PA$_6$MA of $M = 25\,300$ at various temperatures. (b) Temperature dependence of maximum intensity (I_{max}; ●), fwhm (○), and (c) empirical interaction parameter (χ_L).

perature range, since there was no discernible birefringence up to 260 °C. The I_{max} increases and fwhm decreases with increasing temperature (Figures 7b and 8b), which is characteristic of LDOT phase behavior. Consequently, the χ_L's for dPS-*b*-PA$_2$MA and dPS-*b*-PA$_3$MA in Figure 7c and 8c increase with increasing temperature. In fact, χ_L for dPS-*b*-PA$_2$MA approaches a maximum value at temperatures higher than ~220 °C, while χ_L for dPS-*b*-PA$_3$MA shows a weak temperature dependence.[37] It should be noted that χ_L for dPS-*b*-PA$_3$MA becomes negative at temperatures below ~140 °C, which indicates that favorable intermolecular interaction prevails over the free volume effect. In addition, Figure 7c suggests that χ_L for dPS-*b*-PA$_2$MA below ~100 °C is also expected to be negative.

The LDOT phase behavior was also observed for dPS-*b*-PA$_4$MA of $M = 47\,200$, as seen in Figure 9. The SANS profiles show trends similar to those of dPS-*b*-PA$_2$MA and dPS-*b*-PA$_3$MA. However, I_{max} and χ_L increase rapidly at lower temperatures, but not at higher temperatures,[37] which is different from dPS-*b*-PA$_2$MA and dPS-*b*-PA$_3$MA. Such an observation suggests a reversed temperature dependence of I_{max} or χ_L at temperatures above 260 °C, even though the thermal decomposition temperature (T_d) prohibits experimental observation. Thus, a closed-loop phase behavior could occur between T_g and T_d. This speculation was confirmed when the closed-loop behavior for dPS-*b*-PA$_4$MA could be observed by blending with a nonselective solvent of di-*n*-octyl phthalate and a PA$_4$MA-selective solvent of hexadecane.[19] These results suggest that the closed-loop phase behavior is a general phenomenon for weakly interacting block copolymers, especially in the case of LDOT.

Figure 10 shows the SANS profiles for dPS-*b*-PA$_5$MA of $M = 46\,000$, which is reproduced from ref 31. With increasing temperature, I_{max} increases and reaches a maximum and then begins to decrease, whereas fwhm gives the behavior opposite to the temperature dependence of I_{max}. Similarly, χ_L reaches the maximum point at 190 °C, and then decreases with the further increase of temperature.[37]

3.3. Theoretical Consideration. We now compare the experimental results to the Hartree (fluctuation correction) analyses for compressible block copolymer systems.[22,23] Let us consider A-*b*-B diblock copolymers with N_i monomers of *i*-type with a total number of segments, N ($=\sum N_i$). Block copolymer chains are assumed to be perturbed hard sphere chains of uniform diameter σ in a continuum. The nonbonded perturbed *i*,*j*-interactions are characterized by ϵ_{ij}. A hard-core volume

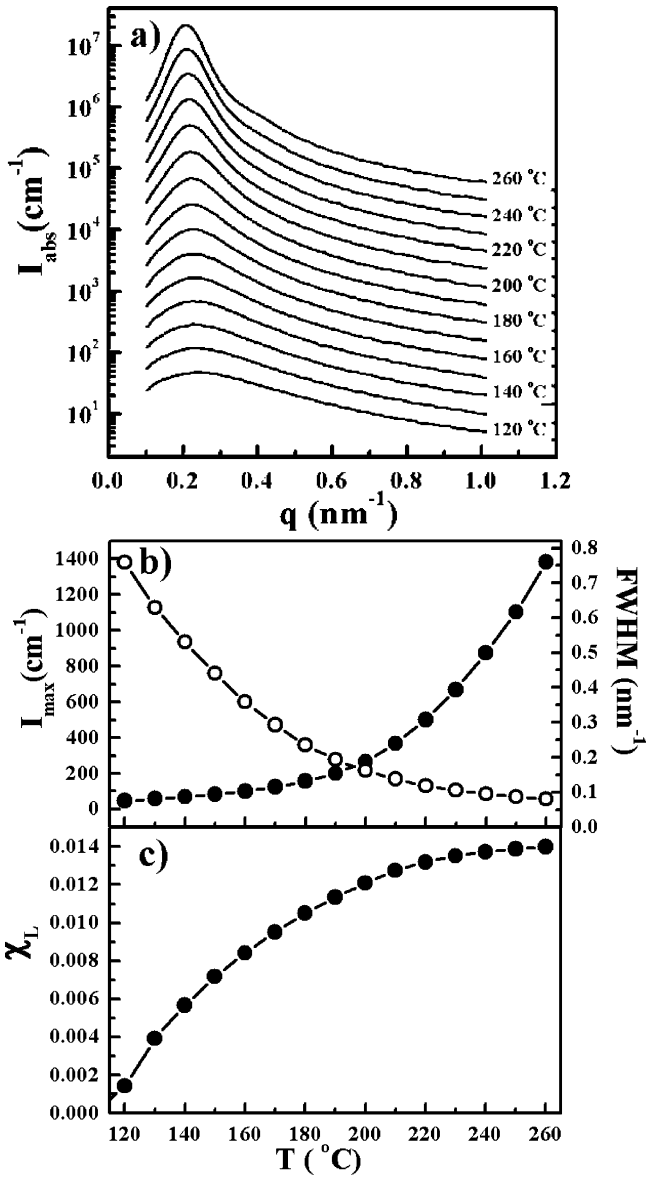

Figure 7. (a) Absolute intensity (I_{abs}) for dPS-*b*-PA$_2$MA of $M = 82\,500$ at various temperatures. (b) Temperature dependence of maximum intensity (I_{max}; ●), fwhm (○), and (c) empirical interaction parameter (χ_L).

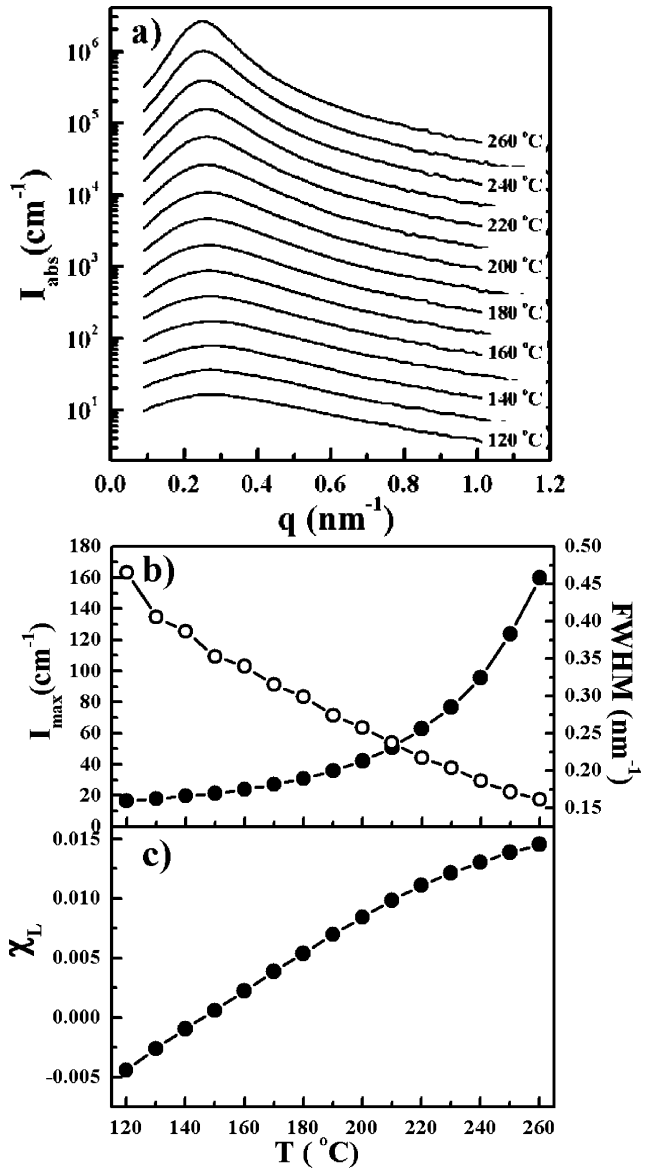

Figure 8. (a) Absolute intensity (I_{abs}) for dPS-*b*-PA$_3$MA of $M = 75\,300$ at various temperatures. (b) Temperature dependence of maximum intensity (I_{max}; ●), fwhm (○), and (c) empirical interaction parameter (χ_L).

fraction of *i*-monomers of the block copolymer chain is defined by $\phi_i \equiv N_i/N$. The fraction of free volume in the system is denoted by η_f and the total packing density, i.e., the fraction of volume occupied by all the monomers, is $\eta = 1 - \eta_f$.

We use a mean-field Landau analysis to study weakly phase segregating block copolymer systems. δF, the difference in free energies between ordered and disordered states, can be expanded in a power series with the thermally averaged order parameters, $\bar{\psi}_1(\vec{r})(\equiv 1/2\eta(\langle\eta_A(\vec{r}) - \eta_A\rangle - \langle\eta_B(\vec{r}) - \eta_B\rangle))$ for ordered profile and $\bar{\psi}_2(\vec{r})(\equiv -\langle\eta_f(\vec{r}) - \eta_f\rangle)$ for free volume, where $\eta_i(\vec{r})$ and $\eta_f(\vec{r})$ are, respectively, the local packing density of *i*-monomers and the local free volume fraction. The δF is then rewritten as a power series in the Fourier transform of $\bar{\psi}_1(\vec{q})$ and $\bar{\psi}_2(\vec{q})$, with the *m*th-order vertex functions $\bar{\Gamma}^{(m)}_{i...j}$ as its coefficients. After $\bar{\psi}_i(\vec{q})$ is written in polar form, a minimization procedure leads to a Landau free energy expansion only in more strongly fluctuating $\bar{\psi}_1(\vec{q})$ with effective vertex terms as its coefficients at a characteristic wave number q^* ($=q^{max}$). The effective quadratic coefficient, denoted as Γ_2', is given by $\Gamma_2' = \eta[2\chi_s - 2\chi_F]$, where χ_s is obtained from the Gaussian *i*,*j*-correlation functions S^0_{ij} as $1/2N \times \sum S^0_{ij}/\det(S^0_{ij})$, and an effective Flory-type interaction parameter χ_F is subdivided into $\chi_F = \chi_{app} + \chi_{comp}$. The former is the density-dependent exchange energy term as $\chi_{app} \propto [\epsilon_{AA} + \epsilon_{BB} - 2\epsilon_{AB}]$. The latter is given as $\chi_{comp} \approx (\pi\sigma^3/6\eta)P_\phi^2/2kTB_T$ for the symmetric copolymer in the long chain limit, where P_ϕ ($= \partial P/\partial\phi)_{T,v}$) and B_T are, respectively, the disparity in equation-of-state properties between constituents and the isothermal bulk modulus.[38]

Block copolymers are known to exhibit concentration fluctuation effects more strongly than polymer blends. In the Landau mean-field picture, diblock copolymers exhibit disorder → bcc → hex → lam as the segregation tendency is strengthened. For a symmetric copolymer with $P_\phi \to 0$, a continuous transition from disorder to lam is predicted. However, real block copolymers with finite sizes show a direct transition from the disordered state to hex or lam, and the continuous transition is never observed. To include such fluctuation effects, the Landau energy is taken as a reference and corrected self-consistently to obtain the Hartree free energy. It is well documented in our previous publications that $N\chi_F(q^*)$ serves a role of relevant parameter in compressible block copolymers.[21,22] On the basis

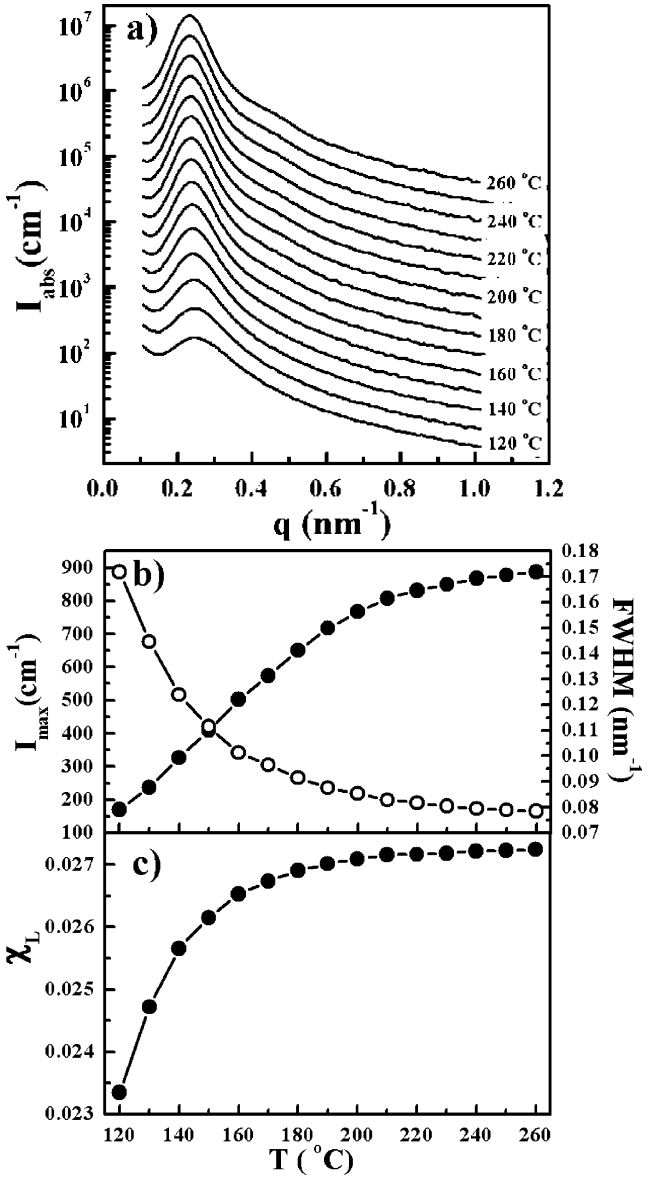

Figure 9. (a) Absolute intensity (I_{abs}) for dPS-*b*-PA$_4$MA of $M = 47\,200$ at various temperatures. (b) Temperature dependence of maximum intensity (I_{max}; ●), fwhm (○), and (c) empirical interaction parameter (χ_L).

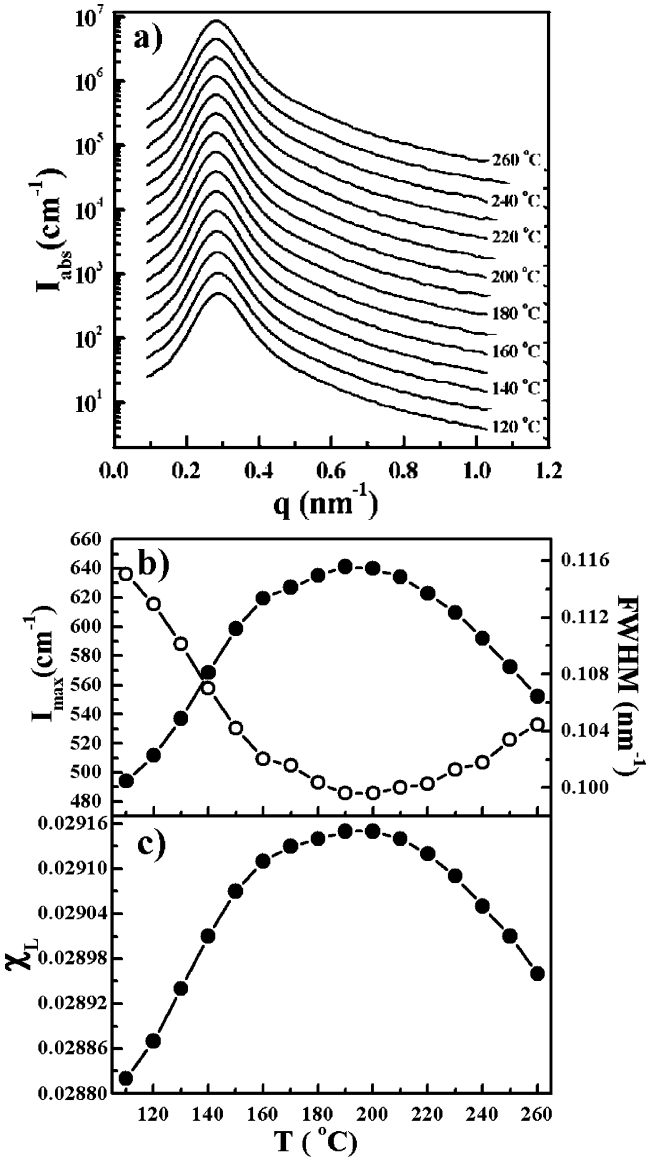

Figure 10. (a) Absolute intensity (I_{abs}) for dPS-*b*-PA$_5$MA of $M = 46\,000$ at various temperatures. (b) Temperature dependence of maximum intensity (I_{max}; ●), fwhm (○), and (c) empirical interaction parameter (χ_L).

of this understanding, it can be easily seen that the mean-field spinodal condition yields $N\chi_F(q^*) = 10.495$ universally for a symmetric copolymer.[21] When the fluctuation effects are considered, our Hartree analysis suggests that $N\chi_F(q^*)$ at the disorder-to-lam ODT for a symmetric copolymer is determined solely by the total chain size N as $N\chi_F(q^*) = 10.495 + 41.022N^{-1/3}$, regardless of the choice of polymer pairs. The fluctuation effects suppress demixing in the mean-field situation.[22]

In treating a block copolymer system with directional interactions, a simple approach devised by ten Brinke and Karasz[39] or by Sanchez and Balasz[23,40] is adopted here. The central concept is to take the A, B cross-contact interaction parameter as a free energy that possesses not only enthalpic but also entropic contributions. The cross-contact interaction ϵ_{AB} is identified as ϵ_{AB}^{ns} without directional interaction but modified by energy increment $\delta\epsilon$ for directional interaction with a Boltzmann counting for such contacts. A symbol d denotes the ratio of the statistical degeneracies of nondirectional and directional cross-contact interactions. The fraction θ of the total number of cross-contacts that are directional is given as $\theta = [1 + d\exp(-\delta\epsilon/kT)]^{-1}$. The free energy ϵ_{AB} per one cross-contact can be suggested as

$$\epsilon_{AB} = \epsilon_{AB}^{ns} + \delta\epsilon - kT\ln[\theta(1+d)] \tag{4}$$

This newly defined free energy parameter ϵ_{AB} now plays the role of a cross-contact interaction in the original formulation.

To describe the phase behavior of dPS-*b*-PA$_n$MA, several molecular parameters for the CS model are required. For the two constituent homopolymers, the requisite molecular parameters include the self-interaction parameter $h_z\epsilon_{ii}$, the model monomer diameter σ_i, and the chain size N_i/M, where h_z denotes the number of nearest nonbonded neighbors around a chosen monomer and M is again the molecular weight. Volume data are usually used to fit those homopolymer parameters. For PS, all the three homopolymer parameters are adjusted to best fit the volume data given by Quach and Simha.[41] In our recent publication, we reported the volume data for PA$_n$MA in the form of the isothermal Padé equation.[23,42,43] However, the monomer diameter of PA$_n$MA is set to that of PS, and then the

Table 3. Molecular Parameters for PS and Homologous PA$_n$MA Series from $n = 2$ to 5

parameters	dPS	PA$_5$MA [a]	PA$_4$MA	PA$_3$MA	PA$_2$MA
σ_i (Å)	4.039	4.039	4.039	4.039	4.000[b]
$h_z\epsilon_{jj}/k$ (K)	4107.0	3680.9	3738.2	3835.1	3867.2
$N_i/M \times \pi\sigma_i^3/6$ (cm^3/g)[c]	0.418 57	0.430 73	0.420 42	0.410 20	0.393 81
$\epsilon_{ij}^{ns}/(\epsilon_{PS}\epsilon_{jj})^{1/2}$		0.982 68	0.976 84	0.983 43	0.980 42
$h_z\Delta\epsilon^{ns}/k$ (K)		146.350	190.167	136.179	159.671
$\delta\epsilon/\epsilon_{PS}$		0.185	0.239	0.180	0.207

[a] The molecular parameters for dPS-*b*-PA$_5$MA are slightly different from those published previously in ref 23 in order to better describe this deuterated sample. [b] This discrepancy in monomer diameter is resolved by adopting the conventional Lorentz mixing rule as $\sigma = (\sigma_1 + \sigma_2)/2$. [c] A composite parameter that yields the ratio of the chain size N_i to molecular weight M.

Table 4. Molecular Parameters for PS and PA$_n$MA for $n = 1$ and 6

	dPS	PA$_1$MA	PA$_6$MA
σ_i (Å)	4.039	4.039	4.120[a]
$h_z\epsilon_{jj}/k$ (K)	4107.0	4388.3	3548.9
$N_i/M \times \pi\sigma_i^3/6$ (cm^3/g)	0.418 57	0.377 57	0.437 71
$\epsilon_{ij}/(\epsilon_{PS}\epsilon_{jj})^{1/2}$ [b]		0.996 80	1.001 28
$h_z\Delta\epsilon/k$ (K)		31.829	10.596

[a] This discrepancy in monomer diameter is resolved by adopting the conventional Lorentz mixing rule as $\sigma = (\sigma_1 + \sigma_2)/2$. [b] No separation of ϵ_{ij} into ϵ_{ij}^{ns} and $\delta\epsilon$ is considered for these ODT systems.

other two parameters are adjusted to best fit the volume data of PA$_n$MA. For simplicity purposes, the CS model assumes the identical diameter for all the monomers in the system. For PA$_n$MA with $n = 2$ and 6, σ_i was set to a slightly different value around that of PS. The conventional Lorentz mixing rule ($\sigma = (\sigma_{PS} + \sigma_{jj})/2$) was used to resolve such discrepancy in monomer sizes. It is not necessary to specify h_z at this stage; the product $h_z\epsilon_{ii}$ suffices for our needs. If all the monomer diameters are identical, then the difference in compressibility between constituents is described solely by the difference in self-interaction parameters ϵ_{ii}'s. A constituent with larger ϵ_{ii} is less compressible. All the homopolymer parameters are listed in Tables 3 and 4. It is seen that PA$_1$MA is the least compressible and PA$_n$MA becomes more compressible as the pendant group size (or n) increases. PS is placed in between PA$_1$MA and PA$_2$MA regarding volume and compressibility.

We now turn our attention to the cross-interaction parameter ϵ_{AB} considered for LDOT systems. The closed loop phase behavior of dPS-*b*-PA$_5$MA was analyzed using the Hartree analysis for compressible block copolymers incorporating directional interactions.[23] This theory was successful in describing the peculiar behavior of dPS-*b*-PA$_5$MA copolymer such as the rarely observed immiscibility loop and its extreme sensitivity to molecular weights and pressure. The origin of the observed loop was attributed to the interactions arising from dipole of phenyl ring and induced dipole of the polar ester group of *n*-pentyl methacrylates.[44,45] The input compressibility difference between the blocks was interpreted to contribute to the pressure sensitivity of the loop. It was shown previously that the plateau of I_{max} in Figure 9 for dPS-*b*-PA$_4$MA as well as the favorable energetics in Figures 7 and 8 respectively for dPS-*b*-PA$_2$MA and dPS-*b*-PA$_3$MA suggests the necessity of directional interaction for these LDOT systems.[46] To describe such directional cross-contacts, it is necessary to know h_z and d explicitly. In dense polymeric liquids, the nearest neighbors surrounding a monomer consist of h_z nonbonded monomers and two bonded monomers. We then choose $h_z \approx 10$, such that it is consistent with the conventional face-centered cubic lattice. The degeneracy ratio d is simply fixed to 11, implying that the directional interaction pair is formed only in the limited range of spatial

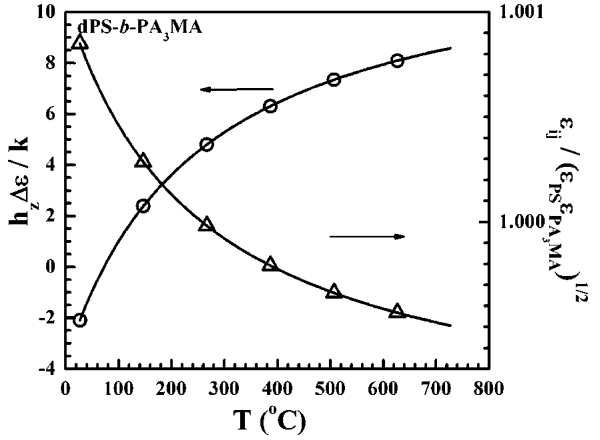

Figure 11. $\Delta\epsilon$ and ϵ_{ij} as a function of temperature for dPS-*b*-PA$_3$MA. Note that ϵ_{ij} varies around Berthelot's rule as $(\epsilon_{PS}\epsilon_{jj})^{1/2}$.

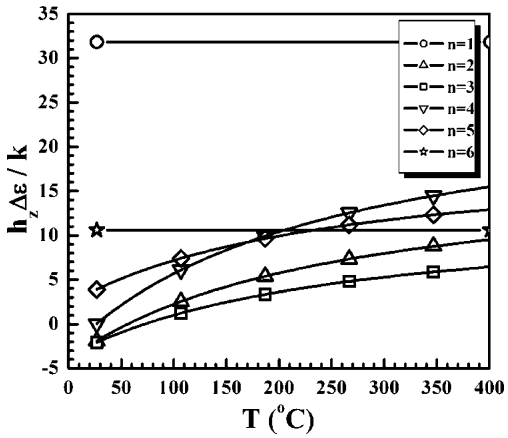

Figure 12. $\Delta\epsilon$ for all the homologous dPS-*b*-PA$_n$MA's as a function of temperature.

arrangements of two dissimilar monomers. The nondirectional part ϵ_{AB}^{ns} and directional part $\delta\epsilon$ of ϵ_{AB} are determined from the experimental ODT's or LDOT's at ambient pressure given in Table 2 for the symmetric dPS-*b*-PA$_n$MA copolymer of the indicated molecular weights. It should be emphasized that the Hartree free energy,[22] not the mean-field Landau energy, is used here to take the fluctuation (finite size) effects into account. The Hartree energy predicts that the copolymer with this size shows a first-order transition from disorder to lamella microdomain, which is indeed the observed behavior.[17] The nondirectional cross-contact interaction is characterized by $\epsilon_{ij}^{ns}/(\epsilon_{PS}\epsilon_{jj})^{1/2}$, which is around 0.98 to yield repulsive $h_z\Delta\epsilon^{ns}/k$ ($= h_z(\epsilon_{AA} + \epsilon_{BB} - 2\epsilon_{AB}^{ns})/k$) from 135 to 190. The directional interaction is adjusted with $\delta\epsilon/\epsilon_{PS}$ of 0.18−0.24. These values are listed in Table 3.[47] Figure 11 demonstrates $\epsilon_{ij}/(\epsilon_{PS}\epsilon_{jj})^{1/2}$ and $h_z\Delta\epsilon/k$ modified with $\delta\epsilon$ for dPS-*b*-PA$_3$MA, where ϵ_{ij} varies around $(\epsilon_{PS}\epsilon_{jj})^{1/2}$, Berthelot's rule, starting with favorable $\Delta\epsilon$ at lower temperatures to end with unfavorable $\Delta\epsilon$ at higher temperatures because of the entropic penalty. For the remaining ODT-type dPS-*b*-PA$_n$MA systems with $n = 1$ or 6, $\delta\epsilon$ is set to zero and $\epsilon_{ij}/(\epsilon_{PS}\epsilon_{jj})^{1/2}$ to ~0.99 without the separation of ϵ_{ij} into ϵ_{ij}^{ns} and $\delta\epsilon$, because in the former case each block may be too rigid to associate/dissociate directional pairs, and in the latter case, it may be harder to sustain directional pairs due to large excluded volume and excess flexibility of the hexyl methacrylate block. These cross interaction parameters are listed in Table 4. We plot $\Delta\epsilon$ as a function of temperature in Figure 12 for the whole series of dPS-*b*-PA$_n$MA. The LDOT systems possess temperature dependent $\Delta\epsilon$, while the remaining ODT systems take the fixed value of $\Delta\epsilon$. The selected $\delta\epsilon$ for the symmetric

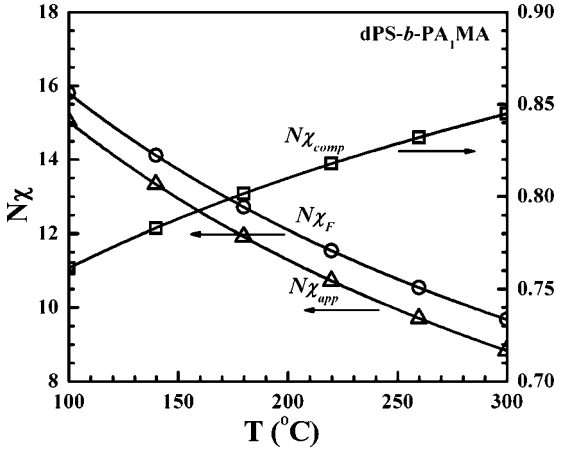

Figure 13. $N\chi_F$ for dPS-*b*-PA$_1$MA of $M = 19\,800$ ($N = 395$). In addition, $N\chi_{app}$ and $N\chi_{comp}$ are drawn together.

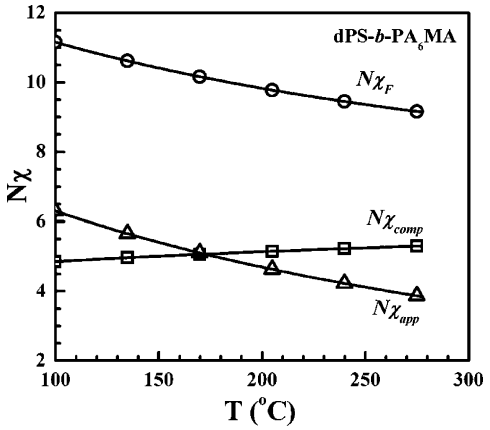

Figure 14. $N\chi_F$ along with $N\chi_{app}$ and $N\chi_{comp}$ for dPS-*b*-PA$_6$MA of $M = 25\,300$ ($N = 506$).

LDOT-type dPS-*b*-PA$_n$MA's yields the energy gain per one monomer ($\propto(h_z\delta\epsilon/2)\phi[1-\phi]\theta$) of ~0.07 kJ/mol with $\theta = \sim 0.1$ at ~130 °C, whereas the cohesive energy per 1 mol of chemical repeating units for each block reaches ~30 kJ/mol.[23]

We discuss first the phase behavior of disordered samples. Figure 13 shows the calculated $N\chi_F$ for the ODT-type dPS-*b*-PA$_1$MA of $M = 19\,800$ ($N = 395$) as a function of temperature. Over ~200 °C, χ_F is linear just as the experimental χ_L in Figure 5c. Here, the unfavorable interaction term in χ_{app} dominates χ_F. For another ODT-type dPS-*b*-PA$_6$MA of $M = 25\,300$ ($N = 506$), the theoretical $N\chi_F$ in Figure 14 is again linear over ~200 °C with a slight downward convexity, while the experimental χ_L in Figure 6c is weakly convex upward. Unlike dPS-*b*-PA$_1$MA, the unfavorable χ_{app} for dPS-*b*-PA$_6$MA is not dominant but balanced with the compressibility term in χ_{comp}, as seen in Figure 14.

More striking features appear in LDOT block copolymers. It is seen either experimentally in Figure 10 or theoretically in Figure 15 that $N\chi_F$ for the symmetric dPS-*b*-PA$_5$MA of $M = 46\,000$ ($N = 940$) exhibits a maximum around 180 (theory) to 190 (experiment) °C, which implies immiscibility loop behavior. This phenomenon is caused by the entropic effects of the input directional interactions. It becomes harder to form directional interaction pairs with increasing temperature, because thermal energy makes the system less amenable to sustain such entropic loss. For dPS-*b*-PA$_n$MA with $n = 2$, 3, and 4, the theoretical $N\chi_F$ exhibits a nonlinear temperature dependence with an upward convexity, as seen in Figures 16−18, which resembles that of dPS-*b*-PA$_5$MA prior to the maximum. The separation of the

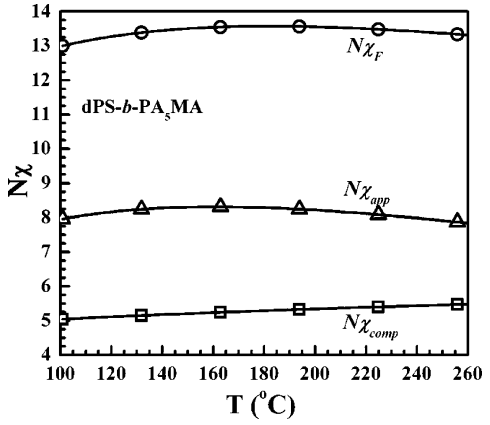

Figure 15. $N\chi_F$ along with $N\chi_{app}$ and $N\chi_{comp}$ for dPS-*b*-PA$_5$MA of $M = 46\,000$ ($N = 940$). It is seen that $N\chi_F$ exhibits a maximum at ~180 °C.

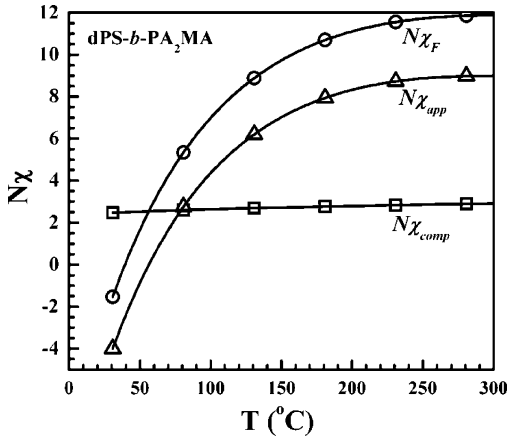

Figure 16. $N\chi_F$ along with $N\chi_{app}$ and $N\chi_{comp}$ for dPS-*b*-PA$_2$MA of $M = 82\,500$ ($N = 1636$).

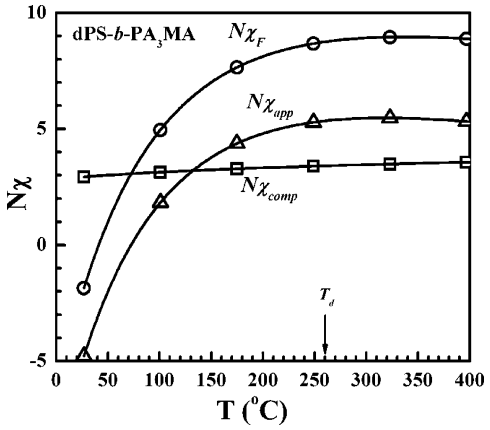

Figure 17. $N\chi_F$ along with $N\chi_{app}$ and $N\chi_{comp}$ for dPS-*b*-PA$_3$MA of $M = 75\,300$ ($N = 1502$). It is seen that $N\chi_F$ below T_d (~260 °C) is only increasing with temperature revealing upward convexity. However, the calculation suggests that $N\chi_F$ indeed possesses a maximum at ~340 °C, which is experimentally inaccessible.

cross interaction ϵ_{ij} into ϵ_{ij}^{ns} and $\delta\epsilon$ was applied to all the LDOT-type series. Therefore, their behaviors should possess many features in common. The difference is where the proposed maximum of $N\chi_F$ is located. If it is placed within the experimentally available temperature range, as in the case of dPS-*b*-PA$_5$MA, then the closed loop behavior is observable. If the maximum is beyond the degradation temperature, then only feature like the upward convexity can be found. The $N\chi_F$ for dPS-*b*-PA$_3$MA in Figure 17 illustrates the general trend. The

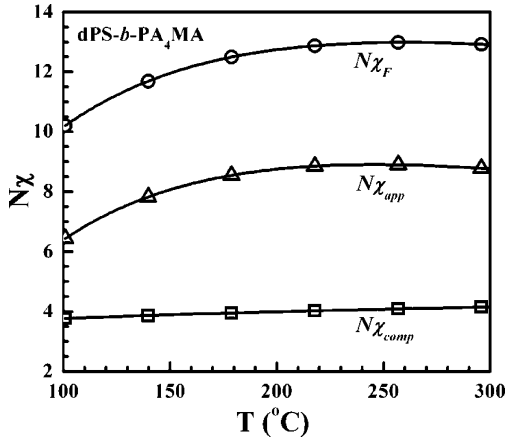

Figure 18. $N\chi_F$ along with $N\chi_{app}$ and $N\chi_{comp}$ for dPS-*b*-PA$_4$MA of M = 47 200 (N = 953). Theory predicts the maximum of $N\chi_F$ at ~260 °C, which is the upper bound of our observation.

experimental χ_L for these materials also shows features similar to that shown in Figures 7−9. The most apparent nonlinearity of $N\chi_F$ and χ_L is observed for dPS-*b*-PA$_4$MA, which implies that the maximum of $N\chi_F$ is quite close to the degradation temperature. In addition, Figures 16 and 17 indicate that $N\chi_F$ for dPS-*b*-PA$_2$MA and dPS-*b*-PA$_3$MA in the lower temperature region is negative, which is driven by the favorable energetics from the directional interactions in χ_{app}. The experimental result also shows that the I_{max} at T < 140 °C for dPS-*b*-PA$_3$MA is lower than that of the correlation hole peak, which implies χ_L < 0.

We now discuss the pressure dependence of the ordering transition temperatures for the block copolymers. The chosen molecular parameters yield the barotropic behavior for PS-*b*-PA$_1$MA but baroplastic behavior for dPS-*b*-PA$_6$MA when we fix $\delta\epsilon = 0$. Such a difference is caused by the relative magnitude of the equation-of-state property disparity. As seen from Table 4, $\epsilon_{PA_1MA} > \epsilon_{PS}$ and $\epsilon_{PA_6MA} < \epsilon_{PS}$, which tells us that PA$_1$MA is less compressible than dPS and PA$_6$MA is more compressible than PS. The difference in self-interactions is smaller for dPS-*b*-PA$_1$MA than for dPS-*b*-PA$_6$MA and, thus, P_ϕ is smaller for the former, while the given sequence of ϵ_{ii} values in Table 4 yields the larger B_T for the former. So, $N\chi_{comp}$ < 0.1 in Figure 13, and $N\chi_{app}$ causes ordering upon pressurization (barotropicity), owing to the increase in the unfavorable contact density with pressure for the dPS-*b*-PA$_1$MA system. In the case of dPS-*b*-PA$_6$MA, a larger $|\epsilon_{PS} - \epsilon_{PA_6MA}|$ contributes to a larger P_ϕ and the more compressible PA$_6$MA yields a smaller B_T, so that $N\chi_{comp}$ reaches ~5, as seen in Figure 14. dPS-*b*-PA$_6$MA then exhibits disordering upon pressurization (baroplasticity), owing to the increase of B_T and decrease of χ_{comp}. The predicted pressure coefficients of the ordering temperatures in Table 5 for those two copolymers with the indicated molecular weights are in agreement with the experimental results in Table 2.

For the LDOT series of dPS-*b*-PA$_n$MA with n = 2 to 5, the selected values of ϵ_{ij}^{ns} and $\delta\epsilon$ predict the closed loop behavior (Table 5), although the upper ODT's of the closed loop are not seen due to the thermal degradation with the exception of dPS-*b*-PA$_5$MA. While the loop for dPS-*b*-PA$_5$MA is extremely sensitive to pressure,[23] other LDOT block copolymers show smaller but still large pressure coefficients of ordering temperatures. It is remarkable that such varied pressure coefficients (Table 2) are well described by the present theory. A relatively large P_ϕ and a diminished B_T because of $[\epsilon_{PS} - \epsilon_{PA_nMA}] \gg 0$ yield $N\chi_{comp}$ ~2 for dPS-*b*-PA$_2$MA to ~5 for dPS-*b*-PA$_5$MA, as shown in Figures 15−18. It is the large value of $N\chi_{comp}$ that produces the strong baroplasticity in these homologues. It should be noted that dPS-*b*-PA$_4$MA has a relatively low value of upper ODT, though it is not observed in experimentally accessible temperature range, due to the strongly nonlinear χ_L in Figure 9c or χ_F in Figure 18 for this block copolymer. A predicted full phase diagram for dPS-*b*-PA$_4$MA at ambient and elevated pressures is given in Figure 19 to depict this situation. It is seen in this figure that the loop size shrinks significantly upon pressurization by the corresponding $\Delta T/\Delta P$.

In summary, we have evaluated molecular parameters for the homologous series of dPS-*b*-PA$_n$MA copolymers based on a compressible Hartree analysis in connection with an off-lattice equation-of-state model. With these parameters, the theory was shown to predict the phase behavior and quantitatively predict the ordering temperatures and their pressure coefficients. It needs to be emphasized that no incompressible theory is capable of predicting peculiar χ_F with such strong convexity and baroplasticity/barotropicity.

As a final comment, we should recognize that the off-lattice CS model does not take disparity in chain flexibility into account. Therefore, the present theory is considered to better work at $T > T_g$ of less flexible block component because otherwise chain flexibility disparity in connection with concentration fluctuations may affect the formation of directional interaction pairs between blocks. This issue is thus left out of our consideration here.

4. Concluding Remarks

The phase behavior and effective interaction parameters (χ_F) of the homologous series of dPS-*b*-PA$_n$MA from methyl (n = 1) to hexyl (n = 6) side groups have been investigated by small-angle neutron scattering (SANS) and a Hartree (fluctuation correction) analysis. Scattering intensities for the block copolymers were measured over a temperature-pressure window to determine phase miscibility, ordering transition temperatures, and their pressure dependence. The χ_F for ODT-type dPS-*b*-PA$_n$MA with n = 1 and 6 decreases with increasing temperature over an extended temperature range. Such behavior of χ_F dramatically changes to a monotonic increase with temperature, resulting in increasing convexity for the LDOT copolymer with increasing n from 2 to 4. This trend is then strengthened to yield a maximum of χ_F, characterizing the closed loop phase behavior for n = 5. Using the Hartree analysis for diblock copolymers, in conjunction with the off-lattice CS equation-

Table 5. Theoretical Transition Temperatures and Their Pressure Coefficients for the Symmetric dPS-*b*-PA$_n$MA's

polymer	M (g/mol)	type	transition (°C) at 0.1 MPa	$\Delta T/\Delta P$ (°C /100 MPa)
dPS-b-PA$_1$MA	22 160	ODT	121	+7
dPS-*b*-PA$_2$MA	99 000	LDOT (+ODT)	225 (-, 412)	+118
dPS-*b*-PA$_3$MA	119 600	LDOT (+ODT)	234 (-, 499)	
	135 000		169 (-,759)	+76
dPS-*b*-PA$_4$MA	55 200	LDOT (+ODT)	170 (-, 398)	+160
dPS-*b*-PA$_5$MA	50 000	LDOT + ODT	134, 244	+730, −1000
dPS-*b*-PA$_6$MA	37 000	ODT	161	−114

[a] The predicted upper ODT's for dPS-*b*-PA$_n$MA (n = 2−4) given inside the parentheses are not observable because of thermal degradation.

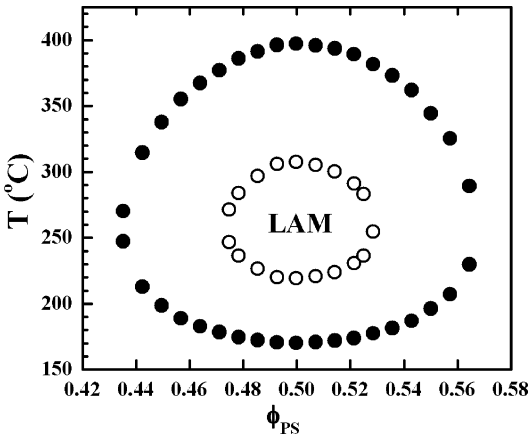

Figure 19. Theoretical phase diagram for dPS-*b*-PA$_4$MA with M = 55 200 at 0.1 (●) and at 30 MPa (○). The concentration fluctuation leads to a first-order transition from disorder to lamellae for the copolymer at the given size. It is notable that dPS-*b*-PA$_4$MA at asymmetric ϕ_{PS} can yield the loop character below the degradation temperature. The loop is shown to shrink significantly by pressurization.

of-state model, proper molecular parameters describing cross-contacts in the given dPS-*b*-PA$_n$MA systems were determined from ordering temperature data. It was shown here that the transition temperatures and their pressure coefficients, as well as χ_F predicted by theory for the homologous copolymer series, are in good agreement with the experimental results. It was argued that directional interactions between dissimilar monomers account for the LDOT and the loop behavior observed in this homologous series of block copolymers.

Acknowledgment. This work has been supported by Korea Science and Engineering Foundation through Hyperstructured Organic Materials Research Center (HOMRC). D.Y.R. acknowledges the Nuclear R&D Programs funded by the Ministry of Science & Technology (MOST) and Seoul Research and Business Development Program (10816) at ICBIN, Korea. J.C. also acknowledges the Nuclear R&D Programs. J.K.K. acknowledges the National Creative Research Initiative Program supported by the Korea Science and Engineering Foundation (KOSEF). T.P.R. acknowledges support from the U.S. DOE office of Basic Energy Sciences. Small-angle neutron scattering was performed at HANARO supported by KAERI, Korea, and at the IPNS of Argonne National Laboratory.

References and Notes

(1) Hadjichristidis, N.; Pispas, S.; Floudas, G. A. *Block Copolymers: Synthetic Strategies, Physical Properties, and Applications*; John Wiley & Sons, Inc.: Hoboken, NJ, 2003.
(2) Hamley, I. W., Ed. *Developments in Block Copolymer Science and Technology*; John Wiley & Sons Ltd.: Chichester, England, 2004.
(3) Bates, F. S.; Fredrickson, G. H. *Annu. Rev. Phys. Chem.* **1990**, *41*, 525.
(4) Leibler, L. *Macromolecules* **1980**, *13*, 1602.
(5) Hashimoto, T. In *Thermoplastic Elastomers*; Holden, G., Legge, N. R., Quirk, R. P., Schroeder, H. E., Eds. Hanser: New York, 1996.
(6) Russell, T. P.; Karis, T. E.; Gallot, Y.; Mayes, A. M. *Nature (London)* **1994**, *386*, 729.
(7) Ruzette, A.-V. G.; Banerjee, P.; Mayes, A. M.; Pollard, M.; Russell, T. P.; Jerome, R.; Slawecki, T.; Hjelm, R.; Thiyagarajan, P. *Macromolecules* **1998**, *31*, 8509.
(8) Mansky, P.; Tsui, O. K. C.; Russell, T. P.; Gallot, Y. *Macromolecules* **1999**, *32*, 4832.
(9) Weidisch, R.; Stamm, M.; Schubert, D. W.; Arnold, M.; Budde, H.; Horing, S. *Macromolecules* **1999**, *32*, 3405.
(10) Hasegawa, H.; Sakamoto, N.; Taneno, H.; Jinnai, H.; Hashimoto, T.; Schwahn, D.; Frielinghaus, H.; Janben, S.; Imai, M.; Mortensen, K. *J. Phys. Chem. Solids* **1999**, *60*, 1307.
(11) Fischer, H.; Weidisch, R.; Stamm, M.; Budde, H.; Horing, S. *Colloid Polym. Sci.* **2000**, *278*, 1019.
(12) Pollard, M.; Russell, T. P.; Ruzette, A.-V.; Mayes, A. M.; Gallot, Y. *Macromolecules* **1998**, *31*, 6493.
(13) Ruzette, A.-V.; Mayes, A. M.; Pollard, M.; Russell, T. P.; Hammouda, B. *Macromolecules* **2003**, *36*, 3351.
(14) Ryu, D. Y.; Lee, D. H.; Kim, J. K.; Lavery, K. A.; Russell, T. P.; Han, Y. S.; Seong, B. S.; Lee, C. H.; Thiyagarajan, P. *Phys. Rev. Lett.* **2003**, *90*, 235501.
(15) Gonzalez-Leon, J. A.; Acar, M. H.; Ryu, S. W.; Ruzette, A.-V.; Mayes, A. M. *Nature (London)* **2003**, *426*, 424.
(16) Gonzalez-Leon, J. A.; Ryu, S. W.; Hewlett, S. A.; Ibrahim, S. H.; Mayes, A. M. *Macromolecules* **2005**, *38*, 8036.
(17) Ryu, D. Y.; Jeong, U.; Kim, J. K.; Russell, T. P. *Nat. Mater.* **2002**, *1*, 114.
(18) Ryu, D. Y.; Lee, D. H.; Jang, J.; Kim, J. K.; Lavery, K. A.; Russell, T. P. *Macromolecules* **2004**, *37*, 5851.
(19) Li, C.; Lee, D. H.; Kim, J. K.; Ryu, D. Y.; Russell, T. P. *Macromolecules* **2006**, *39*, 5926.
(20) Cho, J. *Macromolecules* **2000**, *33*, 2228.
(21) Cho, J. *J. Chem. Phys.* **2003**, *119*, 5711.
(22) Cho, J. *J. Chem. Phys.* **2004**, *120*, 9831.
(23) Cho, J. *Macromolecules* **2004**, *37*, 10101.
(24) Cho, J.; Wang, Z.-G. *Macromolecules* **2006**, *39*, 4576.
(25) Kim, E. Y.; Lee, D. J.; Kim, J. K.; Cho, J. *Macromolecules* **2006**, *39*, 8747.
(26) Freed and co-workers were the first to incorporate finite compressibility into the incompressible RPA by allowing for vacancy. See: (a) McMullen, W. E.; Freed, K. F. *Macromolecules* **1990**, *23*, 255; (b) Tang, H.; Freed, K. F. *J. Chem. Phys.* **1991**, *94*, 1572; (c) Dudowicz, J.; Freed, K. F. *Macromolecules* **1993**, *26*, 213; (d) Freed, K. F.; Dudowicz, J. *J. Chem. Phys.* **1992**, *97*, 2105; (e) Dudowicz, J.; Freed, K. F. *Macromolecules* **1995**, *28*, 6625. Other theories have also been formulated using vacancies as a pseudosolvent in the incompressible treatment. See: (f) Yeung, C.; Desai, R. C.; Shi, A. C.; Noolandi, J. *Phys. Rev. Lett.* **1994**, *72*, 1834; (g) Bidkar, U. R.; Sanchez, I. C. *Macromolecules* **1995**, *28*, 3963; (h) Hino, T.; Prausnitz, J. M. *Macromolecules* **1998**, *31*, 2636. Pair correlation functions and spinodals from the compressible RPA theories were used to explain LDOT behavior driven by the compressibility difference. Our compressible RPA theory is, however, unique in that it does not depend on the widely used pseudosolvent technique.
(27) Cho, J.; Sanchez, I. C. *Macromolecules* **1998**, *31*, 6650.
(28) Russell, T. P.; Hjelm, R. P.; Seegar, P. A. *Macromolecules* **1990**, *23*, 890.
(29) Karis, T. E.; Russell, T. P.; Gallot, Y.; Mayes, A. M. *Macromolecules* **1995**, *28*, 1129.
(30) Ryu, D. Y.; Jeong, U.; Lee, D. H.; Kim, J. H.; Youn, H. S.; Kim, J. K. *Macromolecules* **2003**, *36*, 2894.
(31) Ryu, D. Y.; Lee, D. H.; Jeong, U.; Yun, S.-H.; Park, S.; Kwon, K.; Sohn, B.-H.; Chang, T.; Kim, J. K.; Russell, T. P. *Macromolecules* **2004**, *37*, 3717.
(32) Freed and co-workers presented an incompressible version of their lattice theory.[26a−e] It was argued by them that specific interactions from the differences in the detailed monomer molecular structures can cause LDOT behavior in the diblock copolymers of PS and some PA$_n$-MA's. See: Dudowicz, J.; Freed, K. F. *Macromolecules* **2000**, *33*, 5292. The immiscibility loop was first conjectured by Freed and co-workers for PS-*b*-poly(vinyl methyl ether) in their first ever prediction of LDOT behavior with chosen molecular parameter sets.[26c.]
(33) Ruzette, A.-V.; Mayes, A. M. *Macromolecules* **2001**, *34*, 1894.
(34) Ruzette, A.-V.; Banerjee, P.; Mayes, A. M. *J. Chem. Phys.* **2001**, *114*, 8205.
(35) Yang, H.; Hadziioannou, G.; Stein, R. S. *J. Polym. Sci., Polym. Phys. Ed.* **1983**, *21*, 159.
(36) It is conventional that the experimental χ_L is fitted to a simple expression as $\chi_L = a + b/T$. The linear least-squares fit to the data yields that $\chi_L = 0.026 + 9.74/T$ in absolute temperature scale (K) for dPS-*b*-PA$_1$MA. For another ODT system of dPS-*b*-PA$_6$MA, we follow Qian et al. (see: Qian, C.; Mumby, S. J.; Eichinger, B. E. *Macromolecules* **1991**, *24*, 1655) to use $\chi_L = a + b/T + c\ln T$ instead to cover the slight upward convexity of χ_L, which is still remained to be interpreted. Nonlinear regression routines yield $\chi_L = 0.3053 - 12.70/T - 0.0364\ln T$ for dPS-*b*-PA$_6$MA.
(37) For LDOT-type or loop-forming dPS-*b*-PA$_n$MA, the following equations were determined to represent the experimental χ_L. $\chi_L = 1.6128 - 118.12/T - 0.2194\ln T$ for dPS-*b*-PA$_2$MA; $\chi_L = 0.2694 - 42.18/T - 0.0279\ln T$ for dPS-*b*-PA$_3$MA; $\chi_L = 0.9681 - 64.21/T - 0.1307\ln T$ or $\chi_L = 0.2831 - 374.26/T + 182484.2/T^2 - 2.97/T^3$ for a better fit for dPS-*b*-PA$_4$MA; $\chi_L = 0.1626 - 8.658/T - 0.0187\ln T$ for dPS-*b*-PA$_5$MA.
(38) Cho, J. *Polymer* **2007**, *48*, 429.
(39) ten Brinke, G.; Karasz, F. E. *Macromolecules* **1984**, *17*, 815.
(40) Sanchez, I. C.; Balazs, A. C. *Macromolecules* **1989**, *22*, 2325.
(41) Quach, A.; Simha, R. *J. Appl. Phys.* **1971**, *42*, 4592.

(42) Sanchez, I. C.; Cho, J.; Chen, W.-J. *Macromolecules* **1993**, *26*, 4234.
(43) Cho, J.; Sanchez, I. C. In *Polymer Handbook*, 4th ed.; Brandrup, J.; Immergut, E. H.; Grulke, E. A. Eds. Wiley-Interscience: New York, 1999; p VI/591.
(44) Kim, H. J.; Kim, S. B.; Kim, J. K.; Jung, Y. M. *J. Phys. Chem. B* **2006**, *110*, 23123.
(45) Kim, H. J.; Kim, S. B.; Kim, J. K.; Jung, Y. M.; Ryu, D. Y.; Lavery, K. A.; Russell, T. P. *Macromolecules* **2006**, *39*, 408.
(46) Ruzette, A.-V. *Nat. Mater.* **2002**, *1*, 85.
(47) Cross-interaction parameters, $\epsilon_{ij}/(\epsilon_{PS}\epsilon_{jj})^{1/2}$ and $\delta\epsilon/\epsilon_{PS}$, for deuterated and hydrogeneous PS-*b*-PA_5MA's are set to (0.98268, 0.185) in Table 3 and (0.98318, 0.18) in ref 23, respectively. The former set of parameters yields the loop with 134 and 244 °C for the deuterated sample with $M = 50000$, whereas experiments show 165 and 245 °C for the same sample.[30] Hydrogeneous hPS-*b*-PA_5MA with $M = 49900$ reveals the loop slightly shifted downward with 131 and 224 °C from theory[23] and with 139 and 224 °C from experiment.[17] However, the predicted pressure coefficients of the ODT's are quite similar for the two cases.

MA070754Z